Polymer 51 (2010) 2320–2328

Contents lists available at ScienceDirect

Polymer

journal homepage: www.elsevier.com/locate/polymer

Controllable growth of hydroxyapatite on electrospun poly(DL-lactide) fibers grafted with chitosan as potential tissue engineering scaffolds

Wenguo Cui [a,b], Xiaohong Li [a,c,*], Chengying Xie [c], Jiangang Chen [a], Jie Zou [a], Shaobing Zhou [a], Jie Weng [a]

[a] Key Laboratory of Advanced Technologies of Materials, Ministry of Education, School of Materials Science and Engineering, Southwest Jiaotong University, Chengdu 610031, PR China
[b] Med-X Research Institute, Shanghai Jiao Tong University, Shanghai 200030, PR China
[c] School of Life Science and Engineering, Southwest Jiaotong University, Chengdu 610031, PR China

ARTICLE INFO

Article history:
Received 16 December 2009
Received in revised form
14 March 2010
Accepted 19 March 2010
Available online 27 March 2010

Keywords:
Fibrous composites
Controllable growth
Tissue engineering scaffolds

ABSTRACT

A novel method was exploited to use electrospun poly(DL-lactide) (PDLLA) fibers grafted with chitosan as the induction sites for composite fabrication to suit better the mechanical and biological demands for biomedical applications. The amount of chitosan grafted on the fiber surface could be controlled by the aminolysis time, and the kinetic equations of HA growth were drafted as a function of the incubation time for fibrous scaffolds with different amounts of grafted chitosan. The introduction of amino groups and chitosan on electrospun PDLLA fibers enhanced the cell proliferation due to the improved surface wettability and alleviated dimensional shrinkage. Significantly higher cytoviability and alkaline phosphatase levels were detected on mineralized scaffolds from chitosan grafted fibers than those from aminolyzed fibers, and cells interacted and integrated well with the surrounding fibers. The fibrous nanocomposites should have potential applications as functional coatings on medical devices and as scaffolds for bone tissue engineering.

1. Introduction

Electrospun fibers possess diameter on micro-/nano-meter scale, infinite length and high surface-to-volume ratio, and electrospun fibrous scaffolds have high porosity, tunable pore sizes and three-dimensional structure [1]. Non-woven electrospun nanofibers are architecturally similar to the structure of extracellular matrix (ECM). The loosely bonding between fibers is beneficial for tissue ingrowth and cell migration and well distribution in the whole fibrous mat, which resulted in suitable substrates for wound dressing and tissue engineering [2]. Nanofibers made of synthetic biodegradable polymers, including poly(ε-caprolactone) (PCL), poly(D,L-lactide) (PDLLA), poly(glycolide) (PGA), and poly(lactic-co-glycolic acid) (PLGA), have been well studied as tissue growth scaffolds, and the low mechanical properties and the lack of bioactive signals are the biggest challenges for special applications [3]. Composite fibers, which can be obtained through blending or coaxial electrospinning, show high mechanics through including inorganic particles within electrospun fibers [4], and high bioactivity through introducing apatite on the fiber surface [5]. Electrospun polymeric fibers show the likeness structurally of naturally collagen, therefore, electrospun composite nanofibers, capable of compositionally and structurally emulating the basic building blocks of the naturally mineralized collagen nanofibers, would possess great potential for regeneration of functional bone-like substitutes [6].

In the past few years, attentions have been focused on the fabrication, physical properties, chemical characteristics and biocompatibility of electrospun fibrous composites for bone tissue engineering, which mainly consisted of hydroxyapatite (HA) and biodegradable polymers. Electrospun PDLLA fibers containing β-tertiary calcium phosphate were fabricated through blending electrospinning, and the fibrous composites showed increasing surface hydrophilicity and improvement of cell adhesion and proliferation [7]. But the inorganic particles could not be well-dispersed in the polymer solution because of the incompatibility and very limited or lacking of specific interactions between the organic and inorganic phases. For improving the dispersion of inorganic particles in the polymer solutions, HA nanoparticles have been modified with surfactant of hydroxystearic acid [8], or grafted with low molecular weight PDLLA [9] before blend electrospinning with polymer matrix. The nanoparticles were dispersed uniformly in electrospun fibers at lower HA contents than 4%, and the fibrous composites exhibited higher strength compared with the initial

* Corresponding author at: School of Materials Science and Engineering, Southwest Jiaotong University, Chengdu 610031, PR China. Tel.: +86 28 87634023; fax: +86 28 87634649.
E-mail address: xhli@swjtu.edu.cn (X. Li).

0032-3861/$ – see front matter © 2010 Elsevier Ltd. All rights reserved.
doi:10.1016/j.polymer.2010.03.037

PDLLA fibrous mats and blended HA/PDLLA composites. However, higher HA loading gave rise to problems like compromised electrospinnability and particle aggregation, resulting in the deterioration of mechanical properties as well as unfavorable cellular responsiveness [9].

Attempts have been made to solve problematic issues of the inoculation of HA particles in electrospun fibrous scaffolds. Chen et al. adopted alkaline erosion of electrospun poly(L-lactide) nanofibers, which was used as a matrix for HA mineralization [10]. A plasma surface treatment was applied to clean and activate the electrospun PCL fibers for calcium and phosphate ion grafting, and fibrous scaffolds with bone-like calcium phosphate coatings were achieved [11]. However, controllable growth of HA on fibrous scaffolds with bone-like profile and high contents has not been achieved while maintaining its fibrous and porous structure. We previously applied electrospun nanofibers as the reaction confinement for the fabrication of fibrous composites. PDLLA ultrafine fibers with calcium nitrate entrapment were prepared by electrospinning, and then incubated in phosphate solution to form *in situ* grown HA within fibers [12]. The formation of nanostructured HA and well dispersion of HA particles on the electrospun fibers were determined. But the mechanical properties were not significantly improved because of the polymer degradation in the process of HA growth under weak alkaline conditions.

The development of materials by mimicking the structure and composition of human tissue has long been a major goal in the field of artificial organs or scaffolds for tissue engineering. The biomineralization process mimics the biological mineral growth in natural bone in a simulated body fluid (SBF) with composition similar to that of human blood plasma and under very mild reaction conditions. The resulting carbonated hydroxyapatite was found to be similar to the mineral in the natural bone, having important characteristics, such as low crystallinity and nanoscale sizes, for the reabsorption and remodeling properties in bone [13]. We exploited a novel method for fabricating fibrous composites through biomineralization on electrospun PDLLA fibers with surface modifications. *In situ* growth kinetics were determined using the grafted gelatin as the induction sites for HA nucleation and growth, but the application as scaffolds for bone tissue engineering has not been reached [14]. Chitosan is considered as one of the most attractive natural biopolymer matrices for bone tissue engineering owing to its structural similarity to the glucoseaminoglycan found in bone [15]. Chitosan, which can be degraded by enzymes in the human body, and the degradation product is nontoxic, has been shown to promote growth and mineral rich matrix deposition *in vitro* and *in vivo* [16,17]. However, a major drawback of using chitosan alone for tissue-engineering applications is its enhanced dissolution due to its hydrophilicity along with swelling characteristics. With its very limit usable solvents and intrinsic poor electrospinnability, chitosan was electrospun into nanofibers with other polymers, followed by cross-linking with formaldehyde or glutaraldehyde to improve the fiber stability [18]. Therefore, chitosan was grafted on electrospun PDLLA nanofibers in the current study and exploited as the induction sites to fabricate fibrous composites. The HA content and growth kinetics can be modulated through changing the chitosan content grafted on the surface of electrospun fibers. Osteoblasts of MC3T3-E1 cells were used to evaluate their biological responses upon seeding into the fibrous scaffolds for bone tissue engineering.

2. Experimental section

2.1. Materials

PDLLA ($M_w = 147$ kDa, $M_w/M_n = 1.35$, D/L = 50/50) was prepared by bulk ring-opening polymerization of DL-lactide using stannous chloride as an initiator [19]. The molecular weight was determined by gel permeation chromatography (GPC, waters 2695 and 2414, Milford, MA) using polystyrene as standard. The column used was a Styragel HT 4 (7.8 × 300 mm). The mobile phase consisted of tetrahydrofuran (THF, Fisher Scientific, Fair Lawn, NJ) using a regularity elution at a flow rate of 1.0 ml/min. Chitosan (low molecular weight, brookfield viscosity 20,000 cps, 85% deacetylation) was supplied by the Qingdao Medical Institute (Qingdao, China). Ultrapure water from a Milli-Q biocel purification system (UPI-IV-20, Shanghai UP Scientific Instrument Co., Shanghai, China) was used. All other chemicals and solvents were of reagent grade or better, and purchased from Changzheng Regents Company (Chengdu, China) unless otherwise indicated.

2.2. Preparation of electrospun fibrous scaffolds

The electrospinning setup and process were performed as described previously [20]. Briefly, the electrospinning apparatus was equipped with a high-voltage statitron (Tianjing High Voltage Power Supply Co., Tianjing, China) of maximal voltage of 50 kV. The PDLLA was completely dissolved into acetone, which was added in a 2-ml syringe attached to a circular-shaped metal syringe needle as the nozzle. An oblong counter electrode was located about 12 cm from the capillary tip. The flowing rate of the polymer solution was controlled by a precision pump (Zhejiang University Medical Instrument Co., Hangzhou, China) to maintain a steady flow from the capillary outlet. Electrospun PDLLA fibrous mats were vacuum dried at room temperature for 2 d to completely remove any solvent residue.

2.3. Chitosan grafting on electrospun PDLLA fibers

The surface modification was performed through a similar procedure as previously described [14]. Briefly, electrospun PDLLA fibrous mats were immersed in 0.02 g/ml 1,6-hexanediamine solution in isopropanol at 37 °C for 10 min, followed by rinsing with pure water to remove free 1,6-hexanediamine. The aminolyzed fibrous mats were immersed in 2.0% glutaraldehyde solution for 1 h at room temperature to transform amino groups into aldehyde groups, followed by rinsing with large amount of pure water to remove free glutaraldehyde. The fibrous mats were then incubated in 4 mg/ml chitosan solution in phosphate buffered saline (PBS, pH = 7.4) for 24 h at room temperature. Chitosan grafted fibrous mats were washed with pure water until no free chitosan could be detected in the washing solution.

2.4. Characterization of chitosan grafted fibers

The morphologies of fibrous scaffolds and diameters of electrospun fibers were investigated by scanning electron microscope (SEM, FEI Quanta 200, The Netherlands) equipped with field-emission gun (20 kV) and Robinson detector after 2 min of gold coating to minimize charging effect. The fiber diameter was measured from SEM images with the magnification of 10,000, and five images were used for each fibrous sample. From each image, at least 20 different fibers and 200 different segments were randomly selected and their diameter measured to generate an average fiber diameter by using the tool of Photoshop 10.0 edition [20]. Attenuated total reflectance-Fourier transform infrared spectroscopy (ATR-FTIR, Thermo Nicolet 5700, Madison, WI) was performed to analyze the chemical group transformation, and the spectra were collected over the range of 4000–400 cm^{-1}. Chemical compositions of the fiber surface were determined by X-ray photoelectron spectroscopy (XPS, XSAM800, Kratos Ltd, Britain) using Mg K_α1,2 radiation, and data were processed by using Kratos VISION 2000.

The total acquisition time was 15 min for each sample. The overlapping peaks were resolved by the peak synthesis method, applying Gaussian peak components after Shirley type background subtraction. To clarify the effect of surface modification on the hydrophilicity, a drop of purified water was deposited onto the fibrous mat using a micro-syringe. The water contact angles (WCA) on the fibrous mat were measured on Kruss GmbH DSA 100 Mk 2 goniometer (Hamburg, Germany) followed by image processing of sessile drop with DSA 1.8 software. The final results were obtained by averaging at least five separate runs.

2.5. Determination of the amount of grafted chitosan

The amount of amino groups on the aminolyzed fibers was quantitatively detected using indicator of ninhydrin as described previously [21]. The chitosan amount on the fibrous scaffolds was quantitatively detected after hydrolyzing in hydrochloride solution [22]. Briefly, 20 mg of fibrous mats were hydrolyzed in 2 ml of 6 M hydrochloride solution in a sealed glass tube at 120 °C for 24 h. After removal of hydrochloride at 70 °C, the residues were dissolved in 2 ml pure water, into which 1.5 ml 3.5% (v/v) acetyl acetone/0.33 M sodium phosphate tribasic dodecahydrate and 0.25 M disodium tetraborate decahydrate (98:2) were added. The reaction was kept at 100 °C for 30 min. After cooling to room temperature, 5 ml dye solution was added. The dye solution was prepared by dissolving 0.64 g dimethylaminobenzaldehyde in 6 ml of 12 M hydrochloride solution and then being diluted by 42 ml isopropanol. The absorbance at 528 nm was measured on an ultraviolet–visible spectrophotometer (UV-2550, Shimadzu, Japan). The chitosan content was quantified by referring to a calibration curve obtained with pure chitosan under the same conditions.

2.6. Mineralization process

SBF with the concentrations of Ca^{2+} and PO_4^{3-} ions 1.5 times larger than those of 1.0 SBF was chosen to trigger homogeneous deposition and growth [14]. The electrospun PDLLA fibers, aminolyzed and chitosan grafted fibrous mats were cut into 80 × 80 mm^2 with the thickness of 0.5 mm. Each specimen was immersed in 50 ml of SBF at 37 °C, which was maintained using the thermostated water bath (Taichang Medical Apparatus Co., Jiangsu, China). The suspensions were changed with fresh SBF solution every other day. Upon removal from SBF at predetermined intervals, the fibrous mats were gently rinsed with pure water and dried as above.

2.7. Characterization of mineralized fibers

The morphology and HA dispersion profiles on mineralized fibers were investigated by SEM as described above, and element analysis was carried out by an energy dispersive X-ray analyzer (EDX), which was directly connected to SEM and environmental mode was the same as that of SEM analysis. To investigate the crystalline phase of calcium phosphate precipitates formed on the PDLLA fibers, samples (20 × 20 mm^2) were analyzed with X-ray diffraction (XRD, Philips X'Pert PRO, The Netherlands) over the 2θ range from 20° to 50° with a scanning speed of 0.35° min^{-1}, using Cu-Kα radiation (λ = 1.54060 Å). The diffraction peak broadening due to small crystallites can be semi-quantitatively estimated from the Scherrer equation: $\beta_{1/2} = (K\lambda)/(D\cos\theta)$ [23], where $\beta_{1/2}$ is the full-width at half-maximum in 2 h calculated by the XRD equipment software, K a constant set to 1, λ the X-ray wavelength in Angstroms, D roughly the average crystallite size, and θ the diffraction angle of the corresponding reflex. The HA formation process and the interactions with the fiber matrix were checked by FTIR as described above.

Thermogravimetric analysis (TGA, Netzsch STA 449C, Bavaria, Germany) was employed to determine the actual yield of HA in the composite material. Approximately 10 mg of sample was heated from 20 °C to 500 °C with a heating rate of 10 °C/min in perforated and covered aluminum pans under a nitrogen purge. The electrospun fibrous mats were punched into small strips (70.0 × 7.0 × 0.6 mm^3), and the uniaxial tensile properties were characterized using an all-purpose mechanical testing machine (Instron 5567, Norwood, MA). The stress–strain curves of the fibrous mats were constructed from the load deformation curves recorded at a stretching speed of 0.5 mm/s. Five separate runs were performed for each sample, and the Young's moduli, tensile strength, and elongation at break were obtained from the stress–strain curves.

2.8. Cell seeding onto fibrous scaffolds

Each of fibrous scaffolds of 250–300 μm thickness was cut into small disks (11 mm in diameter), and sterilized by ^{60}Co γ-ray at a dosage of 10 kGy. Prior to cell seeding, each sample was placed in an individual well of a 48-well tissue culture plate (TCP, Costar, Corning, NY), and a sterilized plastic ring-type holder was put on the specimen to prevent floating and soaked with cell culture medium for 12 h. The immortal pre-osteoblastic murine calvaria cell line MC3T3-E1 (CRL-2593, American Type Culture Collection, Rockville, MD) was used in this study, and maintained in α-MEM (Gibco BRL, Rockville, MD) that was supplemented with 10% fetal bovine serum (FBS, Gibco Invitrogen, Grand Island, NY) and 1% penicillin–streptomycin (Sigma, St. Louis, MO). A total of 100 μl cell suspension with the density of 8 × 10^3 cells/ml was carefully seeded onto the surface of each fibrous disk. The cell-seeded scaffolds were incubated at 37 °C in a humidified atmosphere for 2 h to make cells diffuse into and adhere onto the scaffold before the addition of 1.0 ml of culture medium into each well. The cell-seeded scaffolds were replenished with fresh media every 2 d.

2.9. Cell viability, differentiation and morphology analyses

Cell viability was assayed by Cell Counting Kit-8 reagent (CCK-8, Dojindo Laboratories, Kumamoto, Japan). The mechanism behind this assay is that, metabolically active cells react with tetrazolium salt in CCK-8 reagent to produce a soluble formosan dye that can be observed at 450 nm. Briefly, on days 3, 5, and 7 after incubation, cell grown fibrous scaffolds were transferred to another 48-well TCP filled with 400 μl of fresh RPMI1640 (Gibco BRL, Rockville, MD) with 10% FBS in each well. After incubation at 37 °C for 1 h, 40 μl of CCK-8 reagent were added into each well and incubated for 4 h according to the reagent instruction. An aliquot (150 μl) of incubated medium was pipetted into 96-well TCP and read in a spectrophotometric plate reader at 450 nm (Elx-800, Bio-Tek Instrument Inc., Winooski, VT).

The differentiation of precursor cells to osteoblasts was determined by measuring their alkaline phosphatase (ALP) activity. Briefly, after 3, 5 and 7 d culture, the media were removed and the cell grown fibrous scaffolds were washed twice with PBS. Then 100 μl per well of 0.1% Triton X-100 (Amresco, Solon, OH) was used to lyse the cells for 5 min at room temperature. The chromogenic substrate for ALP was 10 mM 4-nitrophenyl phosphate (Roche, Basel, Switzerland) dissolved in water with 0.5 M tris-base (Amresco, Solon, OH) for 60 min. The ALP concentration was determined by kinetic measurement of the absorbance at 405 nm in a spectrophotometric plate reader.

The morphologies of cells grown on fibrous scaffolds were observed by SEM. Briefly, fibrous scaffolds were washed with PBS twice, and then fixed in 2.5% glutaraldehyde for 6 h at 4 °C.

Following three rinses with pure water, the samples were dehydrated through a series of graded ethanol solutions and then freeze-dried. Dry constructs were sputter coated with gold and observed by SEM at an accelerating voltage of 20 kV.

2.10. Statistics analysis

The values were expressed as means ± standard deviation (SD). Whenever appropriate, two-tailed Student's *t*-test was used to discern the statistical difference between groups. A probability value (p) of less than 0.05 was considered to be statistically significant.

3. Results and discussion

3.1. Characterization of chitosan grafted fibrous scaffolds

Electrospun PDLLA mats were composed of bead-free and randomly arrayed fibers with an average diameter of 1.55 ± 0.42 μm (Fig. 1a). Free amino groups were created on electrospun PDLLA fibers through aminolysis process, and chitosan was covalently coupled via Schiff base formation through glutaraldehyde coupling. Fig. 1b shows the morphologies of chitosan grafted fibrous scaffolds with the diameter of 1.62 ± 0.49 μm. The density of surface amino groups on the obtained fibers was about 2.0 ± 0.2 nmol/cm^2 [14], and the amount of grafted chitosan was 60.1 ± 2.3 ng/cm^2 on the surface of electrospun PDLLA fibers. It indicated that chemical groups with lower binding energy, e.g., methyl groups, were enriched on the surface of electrospun PDLLA fibers due to the high voltage of the electrospinning process [24], which resulted in hydrophobic surface. The water contact angles were measured with the sessile drop method, and electrospun PDLLA fibers and chitosan grafted fibers had WCA values of 137.6 ± 3.1° and 0°, respectively.

The electrospun PDLLA fibers grafted with chitosan were analyzed by ATR-FTIR for structural changes of the matrix polymer and by XPS for the chemical group transformation on the fiber surface. As shown in Fig. 2A, strong absorption peaks appeared in the ATR-FTIR spectrum of chitosan grafted fibers at 1600–1700 cm^{-1} ($\nu_{C=O}$ in −CONH−) and 3500–3700 cm^{-1} (ν_{N-H} in $-NH_2$), which were the main peaks of grafted chitosan. Fig. 2B shows the XPS spectra of fibrous mats with chitosan grafted. Electrospun PDLLA fibers displayed two peaks corresponding to C*1s* (284.8 eV) and O*1s* (530.0 eV), as expected. The N*1s* peak of chitosan grafted fibers was attributed to the amine groups and amide bonds of chitosan. The percentages of O*1s*, N*1s* and C*1s* on the fiber surface were also determined. There was a significant increase in the N*1s* concentration from 0 to 2.63% after chitosan immobilization, while the O*1s* decreased from 26.40% to 18.37%.

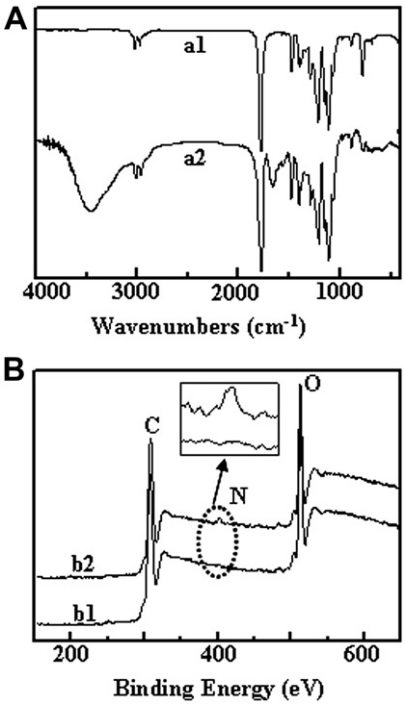

Fig. 2. ATR-FTIR spectra (A) and XPS whole spectra (B) of electrospun PDLLA fibers (a1and b1), and chitosan grafted fibers (a2 and b2) (insets showing the magnified N*1s* peaks).

3.2. Characterization of mineralized fibrous scaffolds

Electrospun PDLLA fibers and chitosan grafted fibers were incubated into SBF to induce calcium phosphate formation. Fig. 3 shows SEM images of electrospun fibers with surfaces precipitates on days 4, 6 and 8 after immersion in SBF. There was no apparent calcium phosphate precipitate formed on electrospun PDLLA fibers during the incubation (Fig. 3a1, a2 and a3), due to the lack of active groups on PDLLA fibers to induce nucleation and growth of calcium phosphate [25]. The growth process of calcium phosphate on the surface of chitosan grafted fibers could be found from few-existent on day 4 (Fig. 3b1), to uniformly dispersed on day 6 (Fig. 3b2) and fully enwrapped around the fiber surface on day 8 after incubation (Fig. 3b3). The exact size of calcium phosphate crystals could not be estimated from SEM images, but it did

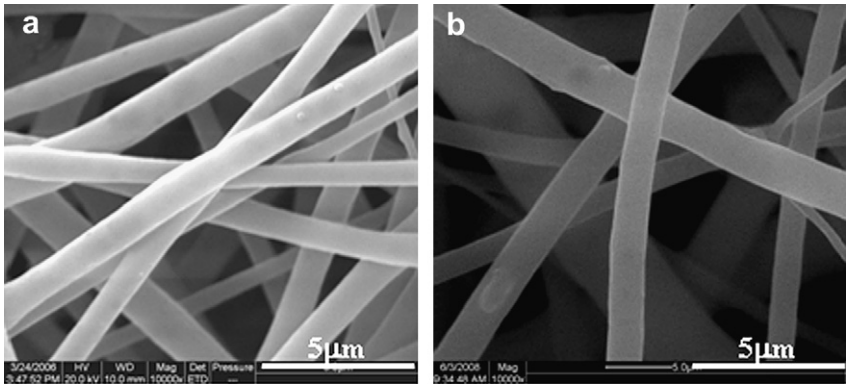

Fig. 1. SEM images of electrospun PDLLA fibers (a) and chitosan grafted fibers (b).

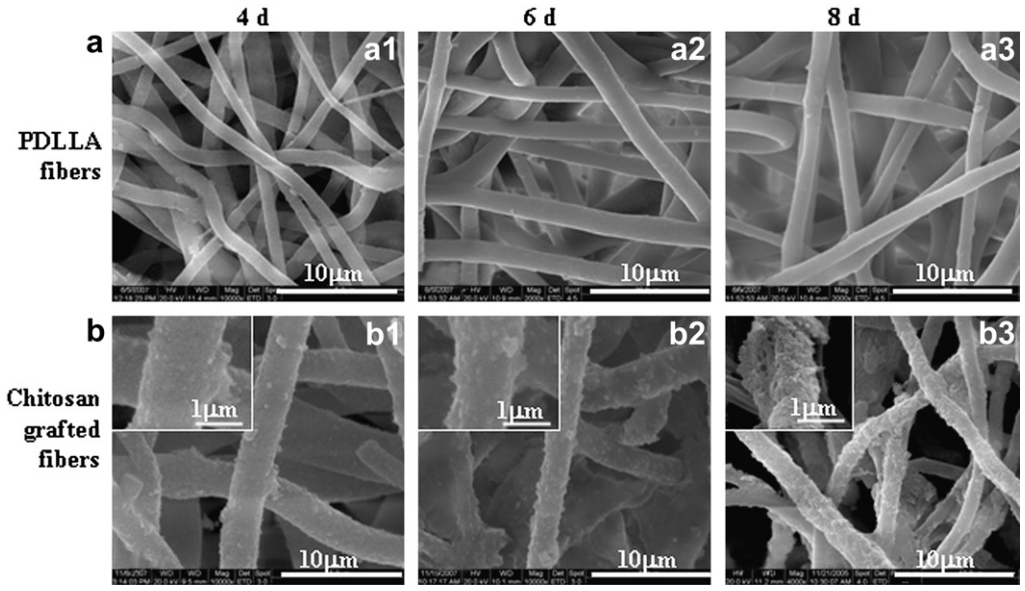

Fig. 3. SEM images of electrospun PDLLA fibers (a) and chitosan grafted fibers (b) after incubation in SBF for 4 (a1 and b1), 6 (a2 and b2) and 8 d (a3 and b3) (insets showing higher magnifications).

appear that the formation of calcium phosphate was made up of very ultrafine particles with the size of below 100 nm, which were homogeneously distributed on the fiber surface.

The formation of calcium phosphate crystals on electrospun fibers was characterized by FTIR, XRD and TG analysis. FTIR spectra of electrospun PDLLA fibers and chitosan grafted fibers after incubation in SBF for 8 d are shown in Fig. 4A. The characteristics of the apatite phase, the ν4 PO_4 bending band at about 600 cm^{-1} and the −OH band at about 3500 cm^{-1}, were present in the FTIR spectra of the composites [12]. There were four vibrational modes theoretically present for phosphate ions: ν1, ν2, ν3, and ν4. The ν1 and ν3 phosphate modes appeared in the region 1200–900 cm^{-1} and another two bands of ν2 and ν4 modes appeared in the region 700–450 cm^{-1} [26]. Fig. 4A, a1 was the typical PDLLA spectrum, and there was no calcium phosphate peak. As seen from the spectra of the formed composite in Fig. 4A, a2, the −OH stretching band at 3572 cm^{-1} belonged to the −OH group along the c-column of HA lattice, and the −OH liberational band were at about 632 cm^{-1}. The

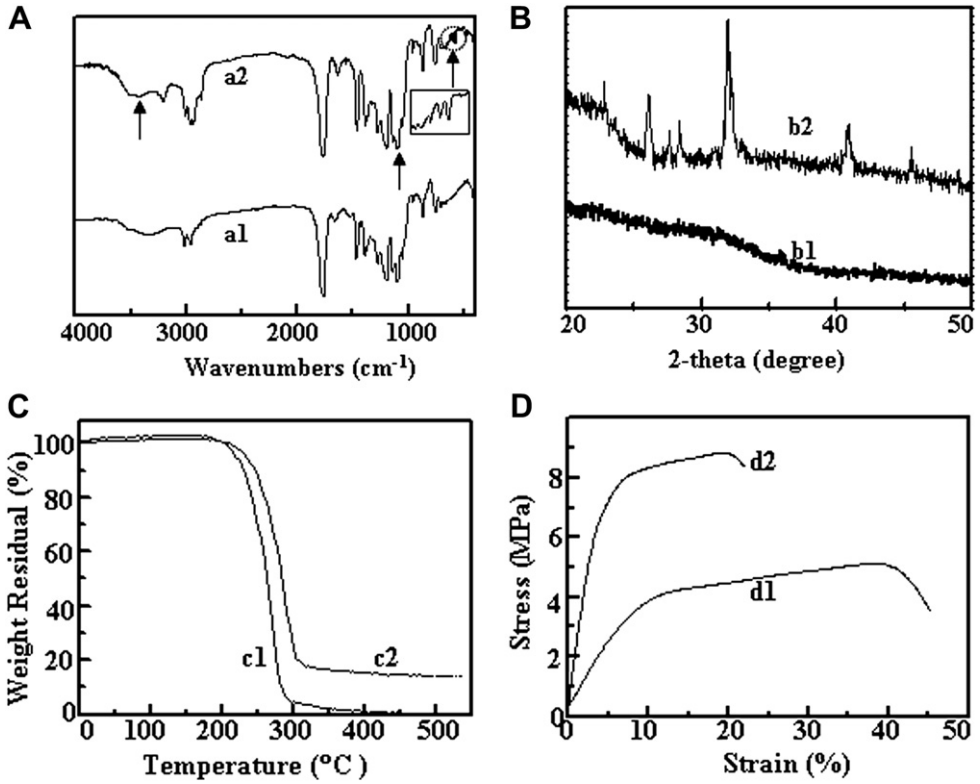

Fig. 4. FTIR spectra (A), XRD patterns (B), TGA curves (C) and stress–strain curves (D) of mineralized scaffolds from electrospun PDLLA fibers (a1, b1, c1 and d1) and chitosan grafted fibers (a2, b2, c2 and d2) after incubation in SBF for 8 d.

broad peak at around 3400 cm^{-1} band was arising from the H–O–H vibration of water molecules absorbed on HA and the fiber surface. The ν3 PO_4 stretching mode at about 1050 cm^{-1} was overlapped by the PDLLA spectrum (Fig. 4A). Phosphate ν4 mode was present in the region of 660 and 520 cm^{-1}, and was well-defined and sharp bands observed in hydroxyapatite. But several sites were detected in this region at 633, 602 and 566 cm^{-1} (inset of Fig. 4A). This splitting of the ν4 vibrational band indicated that the low site symmetry of molecules, as two and three observed bands confirmed the presence of more than one distinction site for the phosphate group [27].

The XRD patterns of electrospun PDLLA fibers and chitosan grafted fibers after incubation in SBF for 8 d are shown in Fig. 4B. No distinct peak appeared for electrospun PDLLA fibers (Fig. 4B, b1). Fig. 4B, b2 shows the XRD profile of mineralized scaffolds from chitosan grafted fibers with a big broad peak centered at $2\theta = 31.8°$, a broad peak at $2\theta = 25.8°$ and smaller broad peaks at $2\theta = 28°$, 42° and 47°, which were characteristic patterns of HA [5]. The broad peaks were seemingly designated as non-stoichiometric HA and low-crystalline apatite phase, which may be a mixture of amorphous calcium phosphate (ACP) and crystalline HA. In the composite there were also other forms of crystalline calcium phosphate phases, such as octacalcium phosphate (OCP), as seen from the XRD patterns of the composite (Fig. 4B, b2) [5]. The crystal size (0 0 2) values (reflection range from 25° to 27°) were related to the crystal size in the wide dimension of the HA crystallites, because this peak was well resolved and showed no interference [28]. The crystal size of HA on mineralized scaffolds from chitosan grafted fibers was calculated by Scherrer's formula, and that was 19.7 nm, which is similar to the apatite crystals found in bone.

To check the component of the formed composite, TGA was conducted on the mineralized mats. As shown in Fig. 4C, pure polymer fibrous membrane lost nearly all the weight with the temperature increasing up to about 350 °C (Fig. 4C, c1). There were about 13.1% of mineral contents for chitosan grafted fibers after incubation in SBF for 8 d (Fig. 4C, c2). The mechanical properties of mineralized scaffolds were detected, and the strain–stress curves are shown in Fig. 4D. It was noted that the composite formed from chitosan grafted fibers had significantly higher tensile strength (8.9 ± 0.3 MPa) than electrospun PDLLA fibers (5.1 ± 0.4 MPa). The Young's moduli were 36.2 ± 5.2 and 104.5 ± 12.7 MPa for mineralized scaffolds from electrospun PDLLA fibers and chitosan grafted fibers, respectively. But the strains at the failure decreased after chitosan grafting, which were 46.1 ± 9.2% and 22.5 ± 4.2%, respectively. The composite formed from chitosan grafted fibers had higher elastic modulus and lower strain at failure, which was explained by the fact that HA minerals rendered the electrospun fiber matrix stiffer and less plastic in its deformation, in a manner which was typical of hard inorganic phases.

3.3. Growth kinetics of HA on chitosan grafted fibrous scaffolds

It is generally held that the initiation of the mineral crystals during mineralization process is caused by heterogeneous nucleation. These above results showed that chitosan grafted fibers were favorable for HA deposition and growth in SBF solution, which demonstrated that the nucleation of nano-HA crystals on the fiber surfaces was critically dependent on the functional groups. Chitosan, a deacetylated derivative of chitin that exists extensively in natural biominerals, is a polysaccharide based on glucosamine and acetylated glucosamine units. Chitosan grafted PDLLA electrospun fibers had the WCA value of 0°, which provided the accessibility of calcium and phosphate ions to the fiber surface. Each repeat unit of chitosan has carbonyl and amino groups, which offered the nucleation sites for HA crystals through binding or chelating with calcium and phosphate ions [29]. In water and weak acid solution containing chitosan, the chitosan took on the positive charges because amino groups of chitosan could attract a proton (H^+) from solution [30]. Phosphate ions were enriched on the amino groups at the calcium complexes, which may be attributed to electrostatic and/or polar interactions. The chitosan grafted fibers were examined by ATR-FTIR spectra after incubation in SBF for 1 d (data not shown). Strong absorption bands around 570–600 cm^{-1} and 1050 cm^{-1} were determined, which were assigned to the stretching and bending vibrations of phosphate groups. The broadening of the band around 1050 cm^{-1} showed the presence of polymer and its interaction with the phosphate groups [31]. The increased ionic activity accelerated the nucleation rate of apatite. Once apatite nuclei were formed, they can grow into a uniform layer by consuming the calcium and phosphate ions from SBF. Therefore, compared with electrospun PDLLA fibers and the aminolyzed fibers [14], chitosan grafted fibers facilitated the deposition and growth of HA, and the composite formation should be affected by the amount of chitosan grafted on electrospun fibers.

The amount of chitosan grafted was determined by the amount of amino groups on the fiber surface, which was dependent on the aminolysis time. At a given concentration of 0.02 g/ml 1,6-hexanediamine solution in isopropanol at 37 °C, the influence of the aminolyzing time on the amount of amino groups was found to be characterized by "S"-shape of sigmoidal kinetic curves and can be described by eq. (1) [32].

$$Y = C_{\max}\left(1 - \left(1 + e^{(t-t_m)/k}\right)^{-1}\right) \quad (1)$$

where Y is the conversion representing the fraction of grafted content, and t is the variable of the aminolysis time, C_{max} is the theoretical maximum value of obtaining results, t_m is the time of maximum growth rate, and k is the apparent rate constant.

In order to quantitatively characterize the effect of the amount of grafted chitosan on HA formation and growth, electrospun fibers were aminolyzed for different time periods. Fig. 5 shows the amount of grafted chitosan versus the aminolysis time, which was plotted using the kinetic model of eq. (1). The results are indicated in eq. (2) with the coefficients of correlation of 0.9975, indicating that the amount of grafted chitosan can be obtained through designing the aminolysis time.

$$Y = 139.53 \times \left(1 - \left(1 + e^{(t-10.38)/2.81}\right)^{-1}\right) \quad \left(R^2 = 0.9975\right) \quad (2)$$

Fig. 6a summarizes the amount of HA for fibrous composites grafted with different amounts of chitosan after incubation in SBF at 37 °C. For quantitative analysis of the HA growth kinetics, the

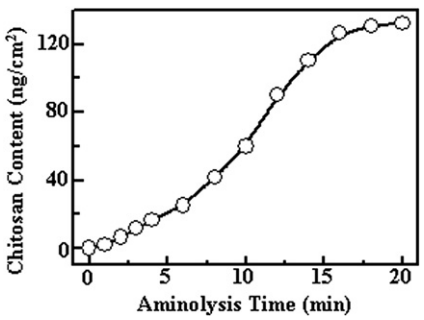

Fig. 5. The amount of chitosan content as a function of the aminolysis time in 0.02 g/ml 1,6-hexanediamine solution in isopropanol at 37 °C.

curves in Fig. 6a were drafted using the kinetic model of eq. (1) for fibers with chitosan contents of 6.6 (eq. (3)), 25.3 (eq. (4)) and 60.1 ng/cm^2 (eq. (5)).

$$Y = 63.18 \times \left(1 - \left(1 + e^{(t-14.35)/3.66}\right)^{-1}\right) \quad \left(R^2 = 0.9998\right) \tag{3}$$

$$Y = 72.40 \times \left(1 - \left(1 + e^{(t-13.78)/3.67}\right)^{-1}\right) \quad \left(R^2 = 0.9996\right) \tag{4}$$

$$Y = 77.65 \times \left(1 - \left(1 + e^{(t-10.72)/3.13}\right)^{-1}\right) \quad \left(R^2 = 0.9993\right) \tag{5}$$

where Y is the HA content formed in the composite (%) and t the incubation time in SBF (d). Higher amount of HA could be found on fibers with higher chitosan contents, and the HA contents could also be controlled by the incubation time. Higher amounts of chitosan may result in higher degrees of binding of calcium and phosphate ions. Moreover, the increased wettability of fibers with higher contents of grafted chitosan should increase the driving force and lower the interfacial energy for HA deposition and growth.

The average Ca/P molar ratio of the mineralized fibrous scaffolds was measured by EDX and the values are shown in Fig. 6b. The Ca/P ratios changed during the process of HA deposition and growth, and high chitosan contents could rapidly induce HA growth and optimize Ca/P ratios close to 1.65. All of the obtained results suggest that the growth of HA on electrospun fibrous mats could be quantitatively controlled by the chitosan content and incubation time.

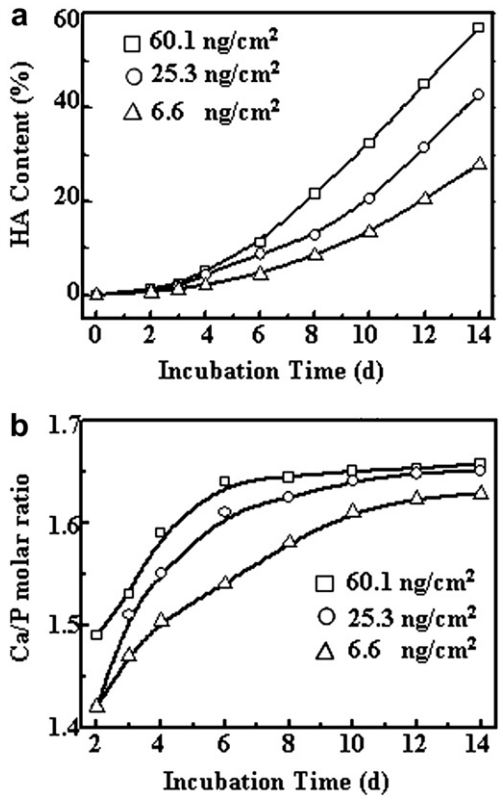

Fig. 6. The amount (a) and Ca/P molar ratio of HA (b) grown on fibrous scaffolds with chitosan contents of 6.6, 25.3 and 60.1 ng/cm^2 after incubated in SBF at 37 °C.

3.4. Cell behaviors on surface modified and mineralized fibrous scaffolds

MC3T3-E1 cells were cultured on the PDLLA fibrous mats, aminolyzed and chitosan grafted PDLLA fibers, mineralized scaffolds from aminolyzed and chitosan grafted PDLLA fibers. Fig. 7a shows the cell viability on days 3, 5 and 7 after incubation. Although PDLLA fibrous scaffolds showed a slow increase in cell proliferation throughout the designated time intervals, it was significantly lower than TCP and other fibrous scaffolds ($p < 0.05$). The introduction of amine groups and chitosan on the electrospun PDLLA fibers enhanced the proliferation rate of MC3T3-E1 cells. There was no significant difference in the cell viability between aminolyzed PDLLA fibers and TCP on days 3, 5 and 7 after incubation ($p > 0.05$). Although the cytoviability on the chitosan grafted PDLLA fibers was not significantly different from aminolyzed fibers on days 3 and 5, it could be significantly enhanced on day 7 ($p < 0.05$). As shown in Fig. 7a, higher proliferation rates were observed for electrospun fibers after mineralization, and significantly higher cell viability was detected on mineralized scaffolds from chitosan grafted PDLLA fibers than those from aminolyzed fibers on day 7 ($p < 0.05$). The osteoblastic differentiation of the MC3T3-E1 cells was investigated by the ALP activities, and the results are summarized in Fig. 7b. On days 3, 5 and 7 after incubation, the ALP activity levels of the mineralized composite scaffolds were significantly higher than those of TCP and unmineralized samples. There was no significant difference in the ALP activity levels between aminolyzed and chitosan grafted PDLLA fibers ($p > 0.05$), while significantly higher ALP levels were detected on mineralized scaffolds from chitosan grafted PDLLA fibers than those from aminolyzed fibers at all time points ($p < 0.05$).

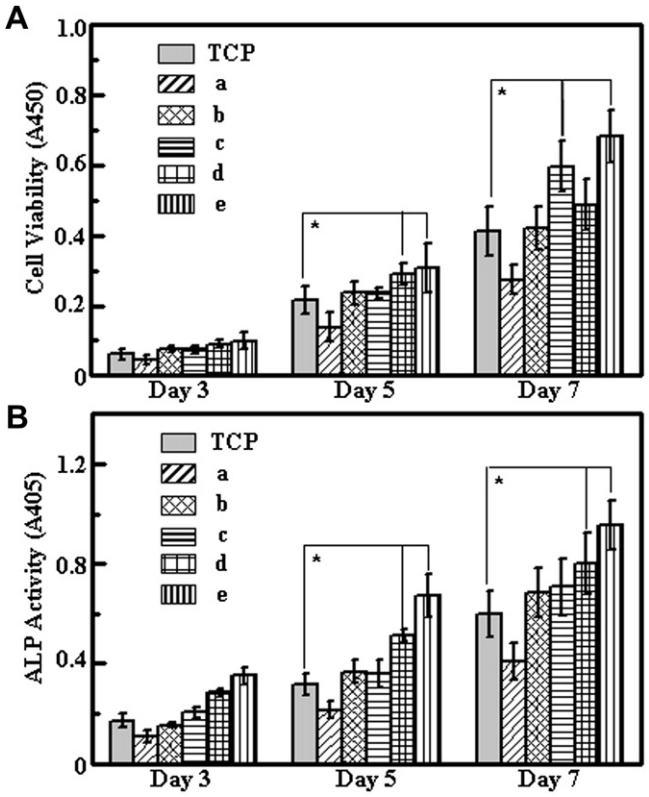

Fig. 7. The proliferation (A) and alkaline phosphatase activity (B) of MC3T3-E1 cells grown on TCP, electrospun PDLLA fibrous scaffold (a), aminolyzed (b) and chitosan grafted fibrous scaffolds (c), mineralized scaffolds from aminolyzed (d) and chitosan grafted fibrous scaffolds (e) after incubation in SBF for 8 d (*$p < 0.05$, $n = 3$).

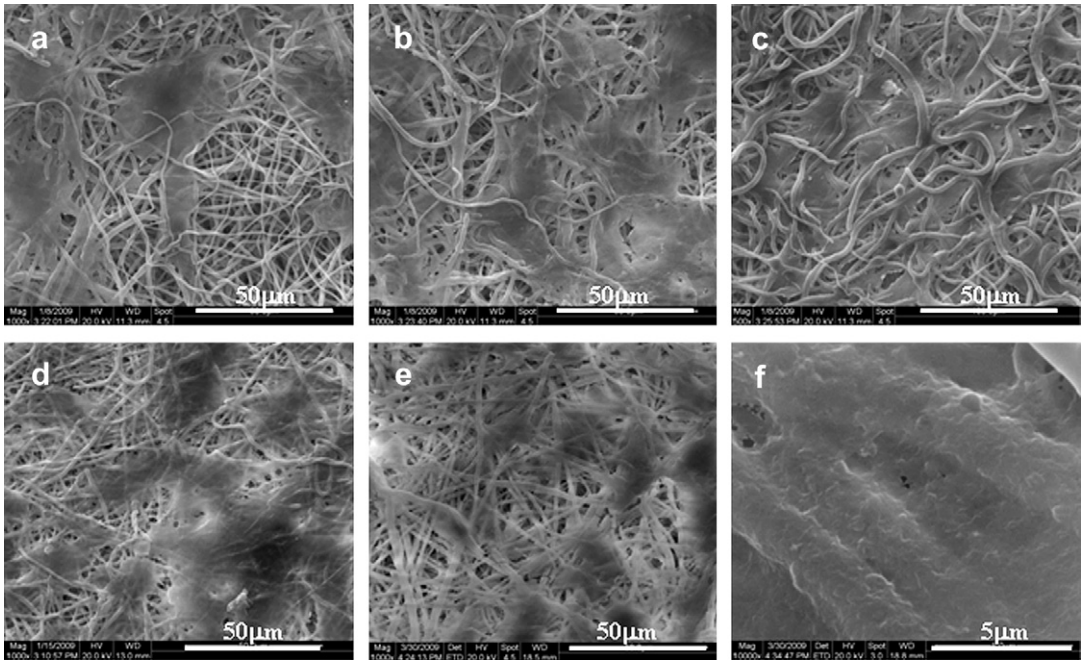

Fig. 8. SEM images of the MC3T3-E1 cells after 7 d culture on electrospun PDLLA fibrous scaffold (a), aminolyzed (b) and chitosan grafted fibrous scaffolds (c), mineralized scaffolds from aminolyzed (d), and chitosan grafted fibrous scaffolds (e and f) after incubation in SBF for 8 d.

Electrospun PDLLA fibers have been widely investigated in a variety of biomedical applications, but the hydrophobic properties hinder the initial biological responses, such as protein adsorption and cell adhesion, limiting their utility as a cell support and tissue regenerating material. As shown in Fig. 7, the cells proliferation and osteogenic activity on the PDLLA fibrous scaffolds were significantly lower than those on TCP ($p < 0.05$). Electrospun PDLLA fibers exhibited a hydrophobic surface with WCA of $132.2 \pm 1.5^{\circ}$. The adhesion and growth of cells on a surface were considered to be strongly influenced by the balance of hydrophilicity and hydrophobicity. Many studies have demonstrated that cells adhere, spread and grow more easily on moderately hydrophilic substrates than on hydrophobic ones [33]. Meanwhile, large dimensional changes (e.g., shrinkage) can occur in electrospun PDLLA fibrous scaffolds [34], which may unfavorably chock the embedded cells in the scaffolds. Therefore, electrospun PDLLA scaffolds were unfavorable for cell attachment, growth and proliferation, and osteoblasts had the least ALP value.

Attempts have been made to improve the cell affinity including coating the surface with natural polymers and making a composite with hydrophilic polymers or with bioactive inorganics [35]. Aminolysis was adopted in the current study to introduce free amino groups onto polyester materials, accompanying with enhancement of their surface hydrophilicity and lower WCA of 106.7° of aminolyzed fibers [14]. In addition, less dimensional shrinkage was detected for aminolyzed PDLLA fibers after incubation into the medium in our experiment. Therefore, the moderate hydrophobicity and alleviated shrinkage of aminolyzed PDLLA fibers could adapt to natural growth and proliferation of cell. Chitosan has a molecular structure similar to that of glycosaminoglycan (GAG) of mammalian connective tissues, which have specific interactions with growth factors and adhesive proteins. In addition, the cationic nature of chitosan and hydrophilic surface of chitosan grafted PDLLA fibrous scaffolds provided an advantage in obtaining a suitable scaffold for cell adhesion in tissue engineering applications. As shown in Fig. 7, significantly higher cell viability could be found on the chitosan grafted PDLLA fibers than on aminolyzed fibers after 7 d incubation.

The current approach modified the surface with an apatite mineral phase, which is considered to have the benefits of not only improving the surface hydrophilicity but also stimulating the osteogenic properties. Compared to those cultured on the unmineralized samples, the ALP activity of cells cultured on the mineralized samples was enhanced at all time points. This can be attributed to the presence of HA nanoparticles on the fiber surface (Fig. 3), which enhanced interactions with pre-osteoblasts, directed cell anchorage and movement, and further regulated bone cell differentiation and matrix syntheses [36]. As shown in Fig. 4B, the formation of non-stoichiometric nanostructured HA was detected in the composite, which may be a mixture of ACP and crystalline HA. Recent studies have described that ACP was beneficial to enhance more bone formation than HA did since the poorly crystalline and amorphous apatites were known to exhibit faster resorption characteristics [37]. The major component of the bone mineral was ACP (65% in young bone and 35% in adult bone), which was a precursor to crystalline hydroxyapatite [38]. The resorbed ACP was replaced by new bone which was mechanically interlocked with the porous scaffold. The degradation of ACP would release Ca and P ions into the surrounding environment, which was found to be responsible for the osteoconductive properties of ACP. As shown in Fig. 7, significantly higher cell proliferation rate and ALP levels were detected on mineralized scaffolds from chitosan grafted PDLLA fibers than those from aminolyzed fibers at all time points. This was attributed to higher apatite contents formed on chitosan grafted PDLLA fibers after mineralization (Fig. 4c), compared to the mineralized scaffolds from aminolyzed fibers [14]. The enhancement of HA growth on chitosan grafted fibers was ascribed to the more hydrophilic surface and the presence of chitosan molecules on the fiber surface, as indicated above.

SEM morphologies of MC3T3-E1 cells cultured on fibrous scaffolds were shown in Fig. 8. Cells were observed spanning the gaps between electrospun fibers, as indicated by the flattened and spreading morphology covering the surface. The cells on the surface modified and mineralized fibrous scaffolds showed the extension of filopodia and anisotropic aggregation of a number of highly spread pre-osteoblasts with morphology that looked similar to viable osteoblasts. A high cell density was observed on the surface of mineralized scaffolds from aminolyzed and chitosan grafted PDLLA fibers. After 7 d culture, the surface of mineralized scaffolds from

chitosan grafted PDLLA fibers was almost covered with cells and possibly mixed with the secreted ECM. The magnified image (Fig. 8f) showed cells conjoined to mineralized fibers, indicating well interaction and integration with the surrounding fibers. All of the obtained results indicated that the mineralized scaffolds acted as an excellent cell support to maintain desirable cell–substrate interactions, to provide favorable conditions for cell proliferation and to stimulate the osteogenic differentiation.

4. Conclusions

Chitosan was grafted on electrospun fibers to induce the deposition and growth of HA crystals. The amount of HA formed on the fibrous composites was controlled through the content of chitosan grafted on the fibers, which could be further determined by the aminolysis process. The mineralized scaffolds from chitosan grafted PDLLA fibers provided favorable conditions for the MC3T3-E1 cells to proliferation, and even stimulated them to undergo osteogenic differentiation. The fibrous nanocomposites should have potential applications as coating materials on medical devices and as scaffolds for bone tissue engineering.

Acknowledgments

This work was supported by National Natural Science Foundation of China (20774075), Program for New Century Excellent Talents in University Funded by MOE (NECT-06-0801), and National Key Project of Scientific and Technical Supporting Programs Funded by MSTC (2006BAI16B01).

References

[1] Agarwal S, Wendorff JH, Greiner A. Polymer 2008;49:5603–21.
[2] Su Y, Li XQ, Tan LJ, Huang C, Mo XM. Polymer 2009;50:4212–9.
[3] Zhu XL, Cui WG, Li XH, Jin Y. Biomacromolecules 2008;9:1795–801.
[4] Gandhi M, Yang H, Shor L, Frank K. Polymer 2009;50:1918–24.
[5] Kim HW, Song JH, Kim HE. Adv Funct Mater 2005;15:1988–94.
[6] Kretlow JD, Mikos AG. Tissue Eng 2007;13:927–38.
[7] Fan HS, Wen XT, Tan YF, Wang R, Cao HD, Zhang X. Mater Sci Forum 2005;75:2379–82.
[8] Deng XL, Sui G, Zhao ML, Chen GQ, Yang XP. J Biomater Sci Polym Ed 2007;18:117–30.
[9] Luong ND, Moon IS, Lee DS, Lee YK, Nam JD. Mater Sci Eng C 2008;28:1242–9.
[10] Chen JL, Chu B, Hsiao BS. J Biomed Mater Res 2006;79A:307–17.
[11] Yang F, Wolke JGC, Jansen JA. Chem Eng J 2008;137:154–61.
[12] Cui WG, Li XH, Zhou SB, Weng J. J Biomed Mater Res 2007;82A:831–41.
[13] Zhang RY, Ma PX. Macromol Biosci 2004;4:100–11.
[14] Cui WG, Li XH, Chen JG, Zhou SB, Weng J. Cryst Growth Des 2008;8:4576–82.
[15] Hu QL, Li BQ, Wang M, Shen JC. Biomaterials 2004;25:779–85.
[16] Iwasaki N, Yamane ST, Majima T, Kasahara Y, Minami A, Harada K, et al. Biomacromolecules 2004;5:828–33.
[17] Kong LJ, Gao Y, Lu GY, Gong YD, Zhao NM, Zhang XF. Eur Polym J 2006;42:3171–9.
[18] Yang DZ, Jin Y, Zhou YS, Ma GP, Chen XM, Lu FM, et al. Macromol Biosci 2008;8:239–46.
[19] Deng XM, Xiong CD, Cheng LM, Xu RP. J Polym Sci Part C 1990;28:411–6.
[20] Cui WG, Li XH, Zhou SB, Weng J. J Appl Polym Sci 2007;103:3105–12.
[21] Zhu YB, Gao CY, Liu XY, Shen JC. Biomacromolecules 2002;3:1312–9.
[22] Lao LH, Tan HP, Wang YJ, Gao CY. Colloids Surf B 2008;66:218–25.
[23] Liao S, Xu GF, Wang W, Watari F, Cui FZ. Acta Biomater 2007;3:669–75.
[24] Cui WG, Li XH, Zhou SB, Weng J. Polym Degrad Stab 2008;93:731–8.
[25] Suh H, Hwang YS, Lee JE, Han CD, Park JC. Biomaterials 2001;22:219–30.
[26] Chang MC, Douglas WH, Tanaka J. J Mater Sci Mater Med 2006;17:387–96.
[27] Rehman I, Bonfield W. J Mater Sci Mater Med 1997;8:1–4.
[28] He QJ, Huang ZL. J Cryst Growth 2007;300:460–6.
[29] Tanaka S, Shiba N, Senna M. Sci Technol Adv Mater 2006;7:226–8.
[30] Zhang FY, Wang J, Hou ZC, Yu M, Xie LD. Mater Des 2006;27:22–426.
[31] Manjubala I, Scheler S, Bossert J, Jandt KD. Acta Biomater 2006;2:75–84.
[32] Swillens S, Dessars B, El Housni H. Anal Biochem 2008;373:370–6.
[33] Arima Y, Iwata H. Biomaterials 2007;28:3074–82.
[34] Cui WG, Zhu XL, Yang Y, Li XH, Jin Y. Mater Sci Eng C 2009;29:1869–76.
[35] Kim HW, Lee HH, Knowles JC. J Biomed Mater Res 2006;79A:643–9.
[36] Yu HS, Hong SJ, Kim HW. Mater Chem Phys 2009;113:873–7.
[37] Habibovic P, Van der Valk CM, Van Blitterswijk CA, De Groot K, Meijer G. J Mater Sci Mater Med 2004;15:373–80.
[38] Klein C, Driessen A, De Groot K, Van den Hooff A. J Biomed Mater Res 1983;17:769–84.